

An Analytical Model for Elucidating Tendon Tissue Structure and Biomechanical Function from *in vivo* Cellular Confocal Microscopy Images

J.G. Snedeker^{a,b} G. Pelled^c Y. Zilberman^c A. Ben Arav^c E. Huber^b R. Müller^b
D. Gazit^{c,d}

^aDepartment of Orthopedics, University of Zürich, Balgrist, and ^bInstitute for Biomedical Engineering, University and ETH Zürich, Zürich, Switzerland; ^cSkeletal Biotechnology Laboratory, Hebrew University – Hadassah Medical Center, Jerusalem, Israel; ^dDepartment of Surgery, International Stem Cell Institute, Cedars Sinai Medical Center, Los Angeles, Calif., USA

Key Words

Functional imaging · Fibered confocal microscopy · Tendon · Biomechanics

Abstract

Fibered confocal laser scanning microscopes have given us the ability to image fluorescently labeled biological structures *in vivo* and at exceptionally high spatial resolutions. By coupling this powerful imaging modality with classic optical elastography methods, we have developed novel techniques that allow us to assess functional mechanical integrity of soft biological tissues by measuring the movements of cells in response to externally applied mechanical loads. Using these methods we can identify minute structural defects, monitor the progression of certain skeletal tissue disease states, and track subsequent healing following therapeutic intervention in the living animal. Development of these methods using a murine Achilles tendon model has revealed that the hierarchical and composite anatomical structure of the tendon presents various technical challenges that can confound a mechanical analysis of local material properties. Specifically, interfascicle gliding can yield complex cellular motions that must be interpreted within the context of an appropriate anatomical model. In this study, we explore the various classes of cellular images that may result from fibered confocal microscopy of the murine Achilles tendon, and in-

roduce a simple two-fascicle model to interpret the images in terms of mechanical strains within the fascicles, as well as the relative gliding between fascicles.

Copyright © 2008 S. Karger AG, Basel

Introduction

In many biological tissues (such as tendon, ligament, and the intervertebral disc), an appropriate material stiffness is essential to proper function. Various imaging techniques have thus been applied in attempts to quantify the mechanical properties of soft tissues *in vivo*. Specifically, ultrasound [Ophir et al., 1991; Skovoroda et al., 1995; Sumi et al., 1995; Wilson et al., 2000; Doyley et al., 2005; Chandrasekhar et al., 2006] and MR elastography [Muthupillai et al., 1995; Chenevert et al., 1998; Lewa et al., 2000; Glaser et al., 2003; Goss et al., 2006; Rouviere et al., 2006; Lopez et al., 2007] have been employed with

Abbreviations used in this paper

2D	two-dimensional
3D	three-dimensional
NCC	normalized cross-correlation

varying degrees of success. The primary limitation to these imaging modalities is either poor spatial resolution that excludes the possibility of identifying ‘microdamage’ (dimensions less than 1 mm) in human tissue, or unsuitability of the method for quantifying certain types of tissues that primarily bear tensile loads.

For instance, at its theoretical limit, ultrasound elastography can attain a spatial resolution of 1.5 mm [Thi-taikumar et al., 2006], but in practice the obtainable resolutions are considerably lower [Chandrasekhar et al., 2006]. On the other hand, using MR elastography with extremely high magnetic fields (11.7 T) and small animals, a relatively fine spatial resolution of $35\ \mu\text{m} \times 35\ \mu\text{m} \times 500\ \mu\text{m}$ has been shown to be possible [Othman et al., 2005], but with the major drawback that MR elastography is only practicable on very soft materials (shear modulus $<50\ \text{kPa}$). This measurable range of stiffness falls below even that of healthy human cartilage (70 kPa), and well below the range of other skeletal tissues such as ligament, bone, tendon, and muscles in tension.

As an alternative imaging modality, endoscopic confocal fluorescence microscopy offers exceptional lateral spatial resolution ($\sim 5\ \mu\text{m}$). The first study describing the application of endoscopic cellular microscopy to derive soft tissue material properties *in vivo* was introduced by Snedeker et al. [2006]. Here tissue biomechanical behavior was quantified by analyzing *in vivo* images of cellular displacements in mouse tendons loaded in tension. All measurements were made using a commercially available endoscopic confocal fluorescence microscope. While the feasibility and reproducibility of the method were established, there were some noted limitations. First, the method requires a minimally invasive surgical procedure to access the tissues of interest. Further, even with optimal configuration of the imaging probe, the maximum potential imaging depth is approximately $200\ \mu\text{m}$, which is sufficient for most small animal tissues, but may not be sufficiently deep to image certain aspects of large animal tissues. Despite these limitations, the method is useful in that it enables the detection of very small mechanical tissue defects ($25\ \mu\text{m}$ or smaller), as well as opening the possibility to simultaneously monitor various aspects of cellular behavior such as apoptosis [Al-Gubory, 2005] or differentiation [Chiu et al., 2006] using fluorescent labeling of specific proteins [Ilyin et al., 2001].

The quantification of tissue strains from cellular displacements in mechanically stretched tendons invokes the classic method of optical elastography: apply a quantified load, measure marker deformations, and infer the tissue strain. Here a load is applied to the tendon, the cells

are used as markers of deformation, and the tissue strain is defined as the relative change in length of the tissue in response to the applied load. For instance, if a tendon fascicle has a length L_0 in an unloaded state and exhibits a change in length of ΔL under load (a positive change indicates tension, negative indicates compression), the so-called ‘nominal’ or ‘engineering’ strain in the fascicle is $\Delta L/L_0$. This yields a dimensionless description of the amount of stretch in the fascicle. When multiple fascicles are imaged under a given mechanical load, the manner with which these loads are distributed among the fascicles can be directly investigated: more heavily loaded fascicles will exhibit higher strains than less loaded fascicles. Similarly, injured or pathological fascicles will often exhibit higher strains than healthy ones due to compromised stiffness and a reduced ability to resist mechanical loads.

In order to extract information about load distribution in the individual tendon substructures, the markers of deformation, in this case fluorescently labeled cells, must be accurately tracked. Thus methods that can uniquely identify individual cells and reliably follow their movements must be implemented. Various computational methods have been proposed for cell tracking, with the vast majority being described for 2-dimensional (2D) cell culture or fluid cell applications [Carter et al., 2005; Ji and Danuser, 2005; Miura, 2005; Yang et al., 2005; Wilson and Theriot, 2006]. Solutions for 3-dimensional (3D) imaging and tracking are more rare, but a few methods have been described [Dufour et al., 2005; Machin et al., 2006; Shi et al., 2006].

In the current study we rely upon a well-established technique for feature tracking called normalized cross-correlation (NCC). Briefly, NCC is a robust, nonparametric texture correlation method that is based on the block search of a grayscale pattern from one frame of a video sequence to the next. For a detailed description of the theory, merits, and shortcomings of NCC as a method for feature tracking and optical elastography the reader is referred to the literature [Duda and Hart, 1973; Goshtasby et al., 1984; Pratt, 1991; Gonzalez and Woods, 2002; Svanbro, 2004; Snedeker et al., 2006].

As we have indicated in previous work [Snedeker et al., 2006], endoscopic images of loaded murine Achilles tendon reflect the complex microanatomy of the tendon. The Achilles tendon is composed of various substructures that work in concert to transfer force from the muscle to the bone [Kannus, 2000]. The functional loading axes of these substructures are not necessarily collinear and vary according to local anatomy as well as to the degree of ankle dorsi/plantar flexion and inversion/eversion. A key limitation of our previous study was the as-

sumption that all tracked cells belonged to the same structure and that all cellular movements were coaxial. This simplifying assumption introduced a considerable source of error in the calculated strain field.

So while the feasibility of using confocal fluorescence endomicroscopy to measure the biomechanical properties of fibrous soft tissue has been established, considerable work remains to be done to make this technology viable for everyday use within either research or clinical environments. First, cellular displacements must be able to be reliably tracked in three dimensions. Soft tissues have a complex anatomical architecture with intricate motions of tissue substructures [Bruehlmann et al., 2004a; Screen et al., 2004] that translate to accordingly complex cellular excursions [Screen et al., 2003; Bruehlmann et al., 2004b]. The results of Snedeker et al. [2006] suggested that an underlying anatomical model must first be developed in order to correctly interpret the *in vivo* movements of imaged cells in response to mechanical load. The present study seeks to address this point by developing an anatomical model of fascicle gliding that can be used to interpret observed cellular motions, and extract the local engineering strain field (quantifying the amount of stretch) within imaged anatomical structures and substructures.

Methods

The following section describes a combined experimental and theoretical approach to developing a model of *in vivo* tendon cell movements. The model is intended to provide a basis for understanding and interpreting images of cell movements in response to functional loading, and can be applied with regard to tracking cell movements and eventually to measuring engineering strains in tendon substructures.

Image Datasets of Cellular Movements in Mechanically Loaded Tendons

A library of image datasets of cellular displacements in mechanically loaded tissues was generated as described in our previous publication [Snedeker et al., 2006]. Briefly, anesthetized, female, C3H/HeN mice aged 10 weeks were placed on the custom loading jig (fig. 1) that was designed and constructed to permit the application of a repeatable load to the Achilles tendon. The femur and tibia of the mouse were physically constrained as a quantified rotational moment was applied to the ankle, resulting in dorsiflexion of the foot and consequent stretching of the Achilles tendon. The relative motions of fluorescently labeled tenocytes in the tendon midsubstance were recorded at 12 frames/s and 5 μm lateral resolution using a Cell-Vizio[®] S-Series endoscopic microimaging system (Mauna Kea Technologies, Paris, France). The 650- μm endoscope tip was held in near contact with the tendon, such that the confocal imaging depth fell just beneath the tendon surface.

The library of video datasets used in the current study was created in a separate investigation of method reproducibility and ex-

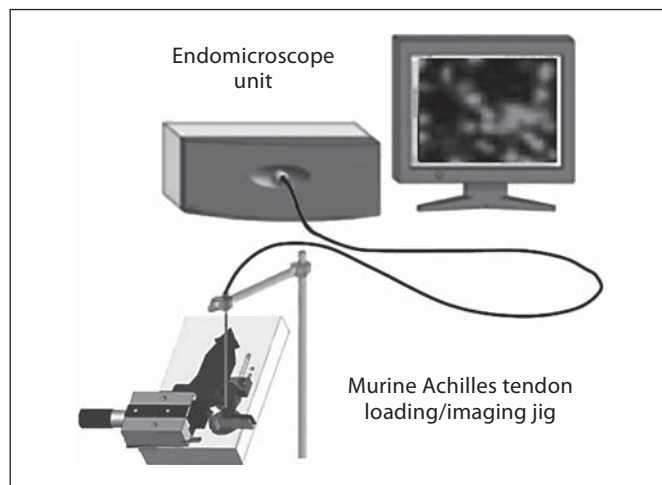


Fig. 1. Schematic representation of the experimental setup with fluorescence endomicroscope and an anesthetized mouse on the Achilles tendon stretching jig.

perimental sensitivity to procedural variability. Here a range of experimental images was generated by perturbing parameters such as the angle of endoscope incidence, the direction of imaging approach (medial, anterior, posterior), and the region of the tendon that was imaged (proximal, middle, distal). For the purposes of the current study – the development of a microanatomical model of tendon structure and function – a quantitative analysis of method variability is not of primary interest and is not presented here. Rather, the resulting image datasets were employed in a qualitative manner to test the capacity of the model to replicate experimentally observed tendon cell excursions, and to introduce these models as a tool for understanding the nature of tendon structure/function from *in vivo* images of tendon under load.

Tracking Cellular Displacements and Quantifying Tissue Strains

For a detailed description and validation of the NCC cell tracking method used in the current project, the reader is referred to our previous publication [Snedeker et al., 2006]. Briefly, NCC-based tracking was implemented within custom software written in Matlab v7.0 (Mathworks, Natick, Mass., USA). In applying NCC to track fluorescently labeled cells, individual cells (or overlapping cells that appear as individual cells) are represented as a 'search pattern' of image grayscale values. To help prevent false positives, the search pattern size is automatically adjusted to include at least one other partial cell. This pattern is then iteratively compared to similarly sized patterns within a search window that encompasses all regions to which the target cell might plausibly move. If an acceptable match is unable to be found (for instance if two previously merged cells separated) the target cell is dropped from the list of tracked cells, and disregarded from further consideration. In the much more common case that the corresponding match is found, interpolation methods are applied to quantify cell displacement with subpixel accuracy (typically on the order of $\pm 0.5 \mu\text{m}$) [Svanbro, 2004; Snedeker et al., 2006].

After the cells have been tracked, cells are clustered according to their shared tendon substructure, here assumed to be fascicles. Clustering is performed automatically by analyzing the individual trajectory of each cell, and grouping them by both the directionality and magnitude of the '2D' cell displacement vectors. Depending upon the interfascicle homogeneity of the displacements and magnitudes, the algorithmic separation of cells into unique fascicles ranges from straightforward to nearly impossible. Therefore, all automatic separations must be verified by visual inspection, which usually confirms immediately whether the cells have been appropriately clustered.

Following cell clustering, fascicle strains and interfascicle gliding can be derived. If the cell density is sufficiently high, it is possible to define the strain field with very high spatial resolution (2.5 times the mean intercellular spacing) [Snedeker et al., 2006]. While high resolution is essential when trying to identify small defects or tears in the tissues, for purposes of the current study we concern ourselves with gross structural behavior of individual fascicles, and therefore have less stringent resolution requirements. Thus we can afford to consider only cells that we can confidently cluster to the same substructure. We then use the trajectories of these cells to determine the functional axis along which the fascicle is stretched (usually taken as the median direction of the clustered cells), and can calculate the engineering strain in the fascicle as the gradient of the cellular displacement field along this functional axis. All automatic calculations of fascicle strain were verified by manual calculations of strain using cellular markers located near the polar ends of the cluster, as is described graphically in figure 2.

An Analytical Model of Tendon Anatomy and Function Using Spring-Mass Models

The complex microanatomy of tendon makes the interpretation of measured cellular movements difficult since a priori knowledge of the underlying anatomy is required to correctly analyze tissue strains. In the current study, we attempt to advance our ability to accurately assess tissue strains by developing a more sophisticated, anatomy-based model to simulate the 3D excursions of fluorescently labeled cells within tendon substructures as they deform under load. To achieve this aim, we implemented a spring-mass model of multiple tendon fascicles under load. The models were used to generate synthetic datasets that mimic actual tissue behavior, and were then preliminarily validated by comparing these synthetic data to cellular images of tendon under load.

The model is based on an assumption that a fibered confocal microscope with a 650- μm objective and a maximum possible tissue penetration depth of 200 μm can simultaneously image no more than two tendon fascicles (which typically have diameters between 100 and 300 μm). The imaged cell excursions will depend on several factors: (1) the depth and angle of incidence of the confocal imaging plane within the tendon structure, (2) the number of fascicles imaged, (3) the orientation of the functional loading axis of the imaged fascicles with respect to the image plane and (4) the material properties of the individual fascicles. The manner in which individual cells contribute to the resulting microscope image is illustrated conceptually in figure 3.

A physics-based model was developed to replicate the cellular displacements that are observed within actual loaded tendon. The cells were assumed to be embedded within tendon substructures,

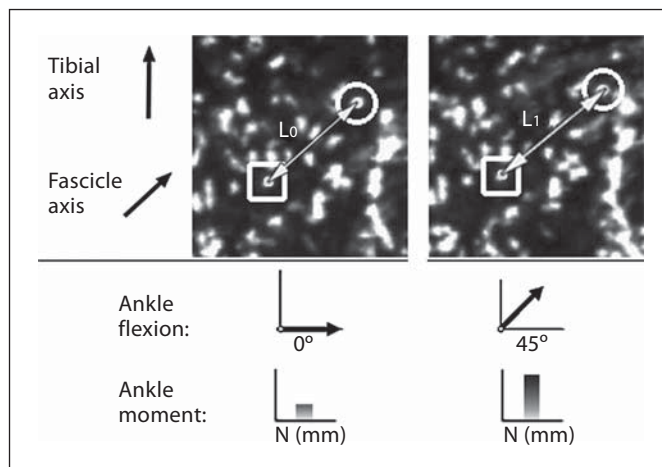


Fig. 2. Cells on individual fascicles are clustered together for analysis, the primary loading axis is identified, and the strain within a fascicle can be verified by measuring the change in length between cells located at polar ends of the cluster.

with cellular motions dictated by the deformations of their host structures. The geometry of the model was considered to consist of two neighboring fascicle segments each with a diameter of 250 μm and a length of 400 μm . Each fascicle was independently assigned a functional axis, along which it was assumed that the fascicle would be loaded in tension, and that it would elongate. To simulate the stretching of these tendon substructures, a spring-mass model was implemented. The two fascicles were discretized into a regular 3D grid, with the nodes of the grid orthogonally connected by springs (fig. 4). The springs were uniformly assigned linearly elastic properties that could be individually tuned to vary local tissue elasticity. More complex connections or material models (nonlinear elasticity, viscoelasticity, localized defects with compromised mechanical competence) were possible, but were not applied for the sake of simplicity. This spring-mass system was then described by a set of simultaneous differential equations combining Newtonian mechanics and Hook's law for linear spring deformation to describe the elastic behavior of a 3D spring-mass grid. These equations were then solved using an iterative approach [Hut et al., 1995] to determine the deformation of the tendon model nodes under an applied external deformation.

The nodal displacements of the numerical models were then used to interpolate the 3D displacement field in response to an applied force boundary condition. Next, 'cells' were uniformly distributed within this 3D field and a virtual imaging focal plane was made to transect the model in a fashion mimicking actual endoscopic measurements. Finally, at incrementally applied load steps, a series of artificial images were created by projecting the cell outlines onto the image focal plane. The cells appeared with an intensity that was inversely proportional to the square of their respective distance from the virtual imaging plane. Thus a sequence of images representing the cell movements in response to incrementally increasing mechanical load was generated.

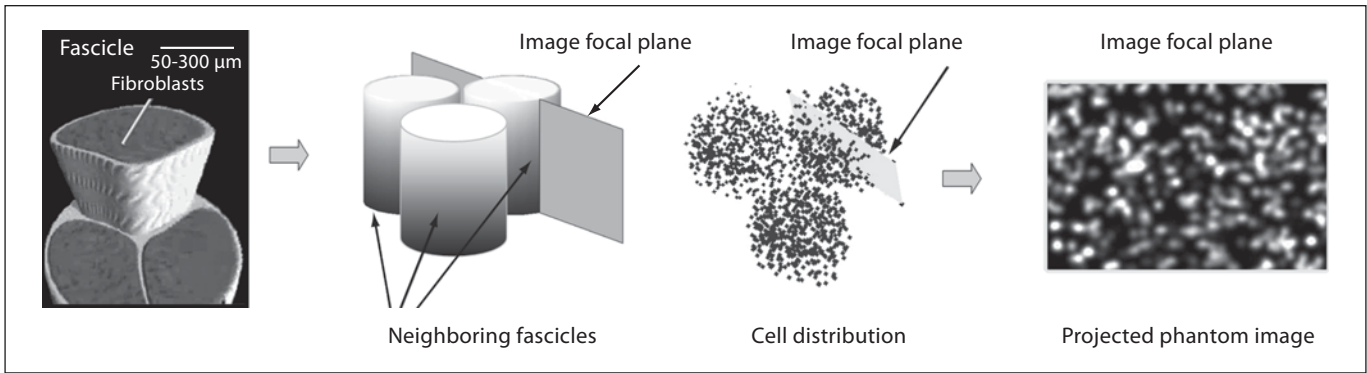
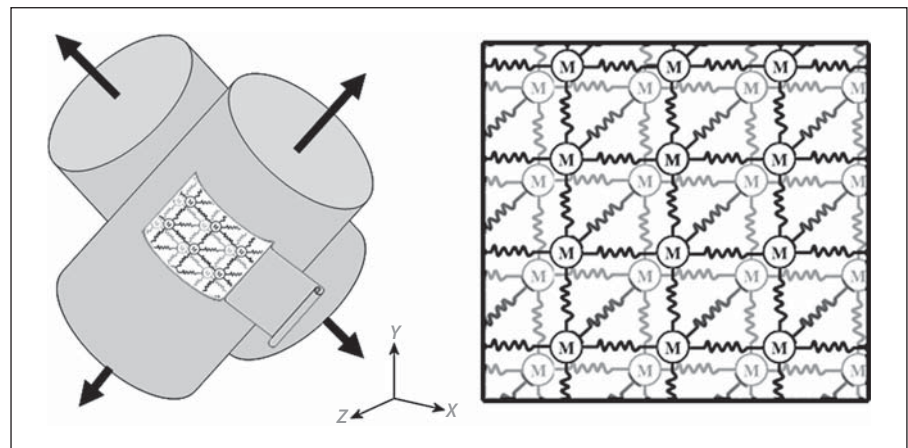


Fig. 3. The proposed 3D physical/anatomical basis underlying *in vivo* tendon cellular image datasets. The confocal imaging plane bisects the tendon structure, and crosses through one or two fascicles depending on the angle of incidence and depth of penetration. Within these fascicles, the fluorescently labeled cells reside in an assumed uniform distribution. The light photons emitted by excited fluorophores are projected onto the image plane, with

an intensity inversely related to relative distance. The result is a composite image of all cells in the vicinity of the confocal imaging plane. As load is incrementally applied to the tendon, the cells will move along the functional axis of the tendon fascicle in which they reside, and this will be reflected in the observed cellular displacements within the image field.

Fig. 4. The spring-mass model has a geometry consisting of two tendon fascicle segments represented by cylinders of a diameter of $250\ \mu\text{m}$ and a height of $400\ \mu\text{m}$. The long, functional axis of the cylinders may be oriented in any direction relative to one another. The cylinder spaces were discretized into an orthogonal matrix of nodes with mass 'M' that are interconnected by linear springs. When the fascicles are loaded in tension, the system deforms, yielding a physically based displacement field from which cell movements can be predicted.



A library of synthetic datasets was created by systematically varying the model. Orientation of the individual fascicles was perturbed, as well as the depth and angle of the incidence of the confocal imaging plane. This library was then cross-referenced against actual images of loaded murine Achilles tendon to qualitatively assess the ability of the synthetic datasets to replicate *in vivo* datasets. Here, each experimentally measured set of *in vivo* cell displacements were tracked, and the individual cell trajectories were grouped according to both the directionality and magnitude of displacement. The synthetic 'cell' trajectories that were generated by the individual model configurations were similarly grouped, and the model configuration that best matched the experimental grouping was selected to represent the experimental trial.

Results

The array of 'virtual' cell displacement datasets from the two fascicle spring-mass model was qualitatively compared to actual *in vivo* images of cell excursions in mechanically loaded murine Achilles tendon. It was determined that nearly all (over 90%) *in vivo* datasets could be effectively reproduced by three basic model cases. The first configuration (fig. 5, case 1) was characterized by the confocal imaging plane falling within a single tendon fascicle. This case mimicked approximately 25% of the *in vivo* image datasets. The second configuration (fig. 5, case 2) represented simultaneous

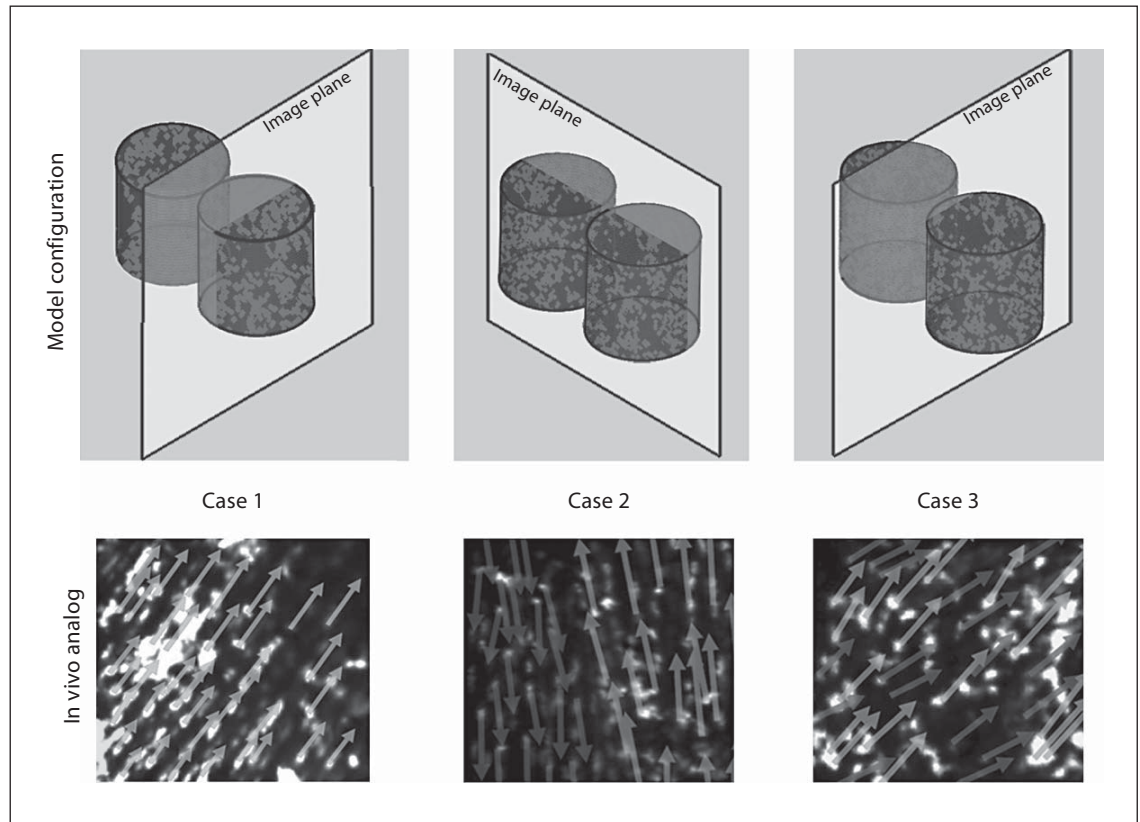


Fig. 5. Three model cases capable of simulating over 90% of the in vivo image dataset library. The arrows superimposed on the in vivo images indicate the displacement vectors of tracked cells. In cases 2 and 3, as the imaging plane bisects multiple fascicles, two subsets of cells are visible.

imaging of cells from two fascicles, with distinct regions of the imaging plane dedicated to each fascicle. This second case corresponded to approximately 20% of the in vivo datasets. The majority of the in vivo data (approximately 50%) were best described by a third configuration (fig. 5, case 3) whereby cells from two fascicles were simultaneously imaged, with cells from both fascicles superimposed and distributed over the entire image field.

After identifying and clustering cells belonging to the same fascicle, it was then possible to calculate the engineering strains within each tendon fascicle, as well as to characterize sliding between neighboring fascicles. This was performed both on the synthetic datasets (where the actual underlying deformation and strain fields were known) and on the in vivo data from stretched murine Achilles tendon. In the synthetic datasets, it was confirmed that deviation of the endoscopic imaging axis from perpendicular to the functional axis of a fascicle

did not affect the accuracy of strain measurement, but did compromise measurement sensitivity and precision. For instance, a 4% reference strain in the fascicle was quantified as $3.9 \pm 0.8\%$ when the angle of the imaging axis was perpendicular to the functional axis of the fascicle, while an incidence angle of 30° yielded a strain measurement of $3.8 \pm 1.5\%$. The ability to accurately quantify fascicle sliding depended more heavily both on the endoscope imaging angle and the anatomical location of the focal plane within the tendon. Specifically, in regions where tendon fascicles are ‘anchored’ (for instance at or near the bony insertion), relative movements between fascicles are less than in certain regions of the tendon midsubstance.

Among the twenty in vivo datasets that were assessed with regard to engineering strain in individual Achilles tendon fascicles (fig. 6), calculated strains ranged between 1 and 5% ($3.2 \pm 1.7\%$, mean \pm SD) at the maximum applied load. Considerable relative move-

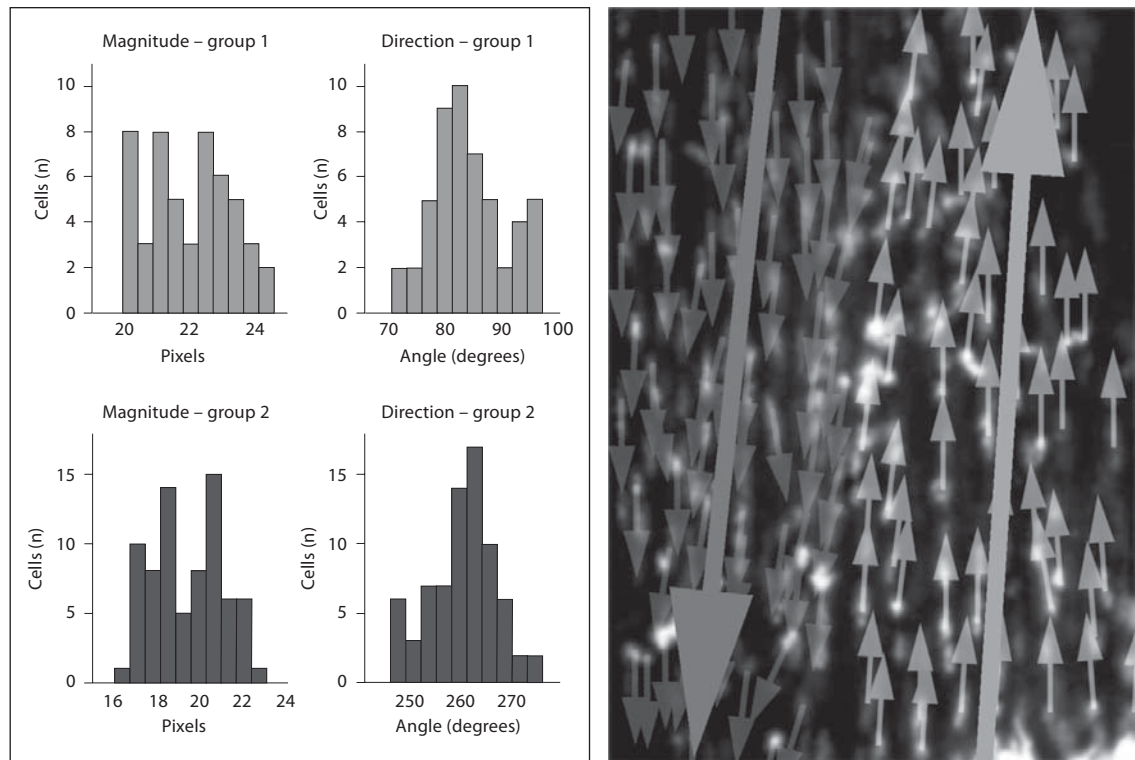


Fig. 6. Clustered cells belonging to two fascicles with cells moving in opposite directions with respect to the imaging probe. Strains calculated within each fascicle are between 3 and 4% while the relative sliding between the fascicles shown here is on the order of 0.2 mm.

ments between neighboring fascicles were observed, sometimes with up to 0.6 mm of relative sliding between juxtaposed fascicles. Again, the magnitude of fascicle sliding was dependent both upon the local anatomy being imaged, and the amount of applied ankle flexion.

In applying automatic NCC cell tracking to the synthetic datasets, certain classes of images could be readily clustered and analyzed (fig. 5, cases 1 and 2), while others proved to be more problematic (fig. 5, case 3). Particularly difficult were instances in which multiple cells were collinearly aligned along imaging axis and appeared as a single cell, only to later emerge as multiple cells (fig. 7). This apparent merging and subsequent separation of individual cells complicated analysis of cell morphology under loading. In cases where single cells were clearly identifiable, cell shape (aspect ratio) appeared to remain unchanged as the tendons were loaded. However, the spatial resolution of the imaging system may not have been sufficiently sensitive to detect modest changes in cell length and width.

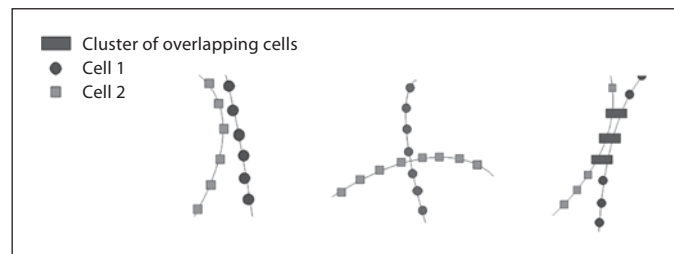


Fig. 7. Individual cells can overlap across several imaging frames, making cell tracking difficult, and inducing potentially large errors into the analysis of mechanical strains.

Discussion

In the present study, we sought to advance a recently developed *in vivo* method for quantifying the local strain field of a living tissue using cells as displacement markers [Snedeker et al., 2006]. In our previous work, certain important technical aspects were identified for improvement.

First and foremost, we attempted to address the serious analytical weakness that is introduced by assuming that all cellular movements are coplanar. Clearly, due to the complex hierarchical anatomy of the tendon, imaged cells do not necessarily belong to the same structure, and analysis based on this assumption yields unsatisfying (inaccurate) results. In order to minimize analytical errors when interpreting the cellular excursions, a more sophisticated model of the underlying local anatomy was required.

To this end, a deformable, two-fascicle model was introduced that is capable of replicating the large majority of the *in vivo* cellular microscopy datasets that we have collected. This model not only generates synthetic data that is essential in developing and testing cell tracking methods, but also provides an anatomical and physical context for making sense of experimental endoscopic images at hand. The model is able to explain the relative movements of individual cells, and provides a physical basis for elucidating the mechanical strains within individual fascicles, as well as for quantifying interfascicle sliding to better understand how the relative movement between individual tendon fascicles is fundamental to proper biomechanical function. As has been indicated in *ex vivo* experiments on rat tail tendon [Screen et al., 2004, 2005] and the intervertebral disc annulus fibrosus [Bruehlmann et al., 2004a, b], relative sliding between collagen fibers can be considerable, and may in fact dominate the biomechanical behavior of collagenous soft tissues. This may help to explain why various tendons of the body, while composed of similar fundamental molecular building blocks (type I collagen, proteoglycans), can have such diverse structural properties that are optimized according to functional demands [Rumian et al., 2007].

Fibered confocal microscope images of loaded tendon produce a series of 2D images that contain encoded 3D information, and efforts to treat this data as 2D can yield spurious analysis of tissue strains [Snedeker et al., 2006]. The proposed model marks a first step in moving past a purely 2D treatment of *in vivo* cellular elastography data. It provides the ability to account for cells on structures that form oblique angles to the confocal imaging plane which move into and out of the field of view over the course of an applied mechanical load. This is important, since large angles between the confocal plane and the actual 3D trajectory of the cell can translate to a considerable source of error in quantifying absolute cell displacement. A micro-anatomy-based model is a critical first step in implementing more precise (3D) cell tracking, and improving the accuracy of the subsequent engineering analysis. With a well-defined anatomical model and accurately tracked cell

displacements, material parameters of the component structures can be extracted and systemic behavior can be predicted over a wide physiological range of tissue loads.

Of course, the end goal is to characterize the material properties of the tissues under investigation. In nondestructive tests, this usually means that the apparent modulus (stiffness) of the material is to be established. While imaging-based technologies can be harnessed to identify the strain field, little can be said about the corresponding material properties without knowledge of the load distribution in the imaged structure. In the case that a quantified loading boundary condition is applied, and the geometry/anatomy of the system is well defined, only then does it become possible to relate the observed strain field to the underlying material properties. One powerful method for establishing the material properties of tissues under load is the inverse finite element method [Van Houten et al., 1999; Plewes et al., 2000; Kauer et al., 2002], by which measured tissue displacements are used as nodal input within finite element models that can predict tissue behavior under a comprehensive range of physiological loading conditions. In later, more sophisticated models of tendon, the mechanical interplay of intertwined tendon substructures could be quantified, and the effects on tissue behavior could be examined in response to more complex loading conditions, such as compression due to wrapping around bony surfaces. Such models using endoscopic cellular microscopy are currently under development, and the present study represents a major enabling step in realizing these models.

These advancements will bring us closer to a viable, high-resolution, minimally invasive technique for the biomechanical analysis of soft tissues *in vivo*. Aside from basic research into skeletal tissue structure and function, such a tool could drastically improve the efficiency of novel clinical therapy development. We envision that fibered confocal fluorescence microscopy will soon be used for the screening of various drugs, proteins, and cell-based approaches to human tissue repair. While the technical limitations of this imaging modality (restricted depth of tissue penetration) may restrict the method to use in preclinical small animal studies, the method may also eventually find applicability in human tissues for which surface loads are of primary interest, such as blood vessel walls or articular cartilage.

Acknowledgments

This work was supported by the EU project 'Adult mesenchymal stem cell engineering for connective tissue disorders. From the bench to the bed side' (GENOSTEM, LSH-2003-503161).

References

- Al-Gubory, K.H. (2005) Fibered confocal fluorescence microscopy for imaging apoptotic DNA fragmentation at the single-cell level in vivo. *Exp Cell Res* 310: 474–481.
- Bruhlmann, S.B., P.A. Hulme, N.A. Duncan (2004a) In situ intercellular mechanics of the bovine outer annulus fibrosus subjected to biaxial strains. *J Biomech* 37: 223–231.
- Bruhlmann, S.B., J.R. Matyas, N.A. Duncan (2004b) ISSLS prize winner: collagen fibril sliding governs cell mechanics in the annulus fibrosus: an in situ confocal microscopy study of bovine discs. *Spine* 29: 2612–2620.
- Carter, B.C., G.T. Shubaita, S.P. Gross (2005) Tracking single particles: a user-friendly quantitative evaluation. *Phys Biol* 2: 60–72.
- Chandrasekhar, R., J. Ophir, T. Krouskop, K. Ophir (2006) Elastographic image quality vs. tissue motion in vivo. *Ultrasound Med Biol* 32: 847–855.
- Chenevert, T.L., A.R. Skovoroda, M. O'Donnell, S.Y. Emelianov (1998) Elasticity reconstructive imaging by means of stimulated echo MRI. *Magn Reson Med* 39: 482–490.
- Chiu, P.W., H. Inoue, H. Satodate, T. Kazawa, T. Yoshida, M. Sakashita, S.E. Kudo (2006) Validation of the quality of histological images obtained of fresh and formalin-fixed specimens of esophageal and gastric mucosa by laser-scanning confocal microscopy. *Endoscopy* 38: 236–240.
- Doyle, M.M., S. Srinivasan, S.A. Pendergrass, Z. Wu, J. Ophir (2005) Comparative evaluation of strain-based and model-based modulus elastography. *Ultrasound Med Biol* 31: 787–802.
- Duda, R.O., P.E. Hart (1973) *Pattern Classification and Scene Analysis*. New York, Wiley.
- Dufour, A., V. Shinin, S. Tajbakhsh, N. Guillen-Aghion, J.C. Olivo-Marin, C. Zimmer (2005) Segmenting and tracking fluorescent cells in dynamic 3-D microscopy with coupled active surfaces. *IEEE Trans Image Process* 14: 1396–1410.
- Glaser, K.J., J.P. Felmlee, A. Manduca, R.L. Ehman (2003) Shear stiffness estimation using intravoxel phase dispersion in magnetic resonance elastography. *Magn Reson Med* 50: 1256–1265.
- Gonzalez, R.C., R.E. Woods (2002) *Digital Image Processing*. Upper Saddle River, Prentice Hall.
- Goshtasby, A., S.H. Gage, J.F. Bartholic (1984) A 2-stage cross-correlation approach to template matching. *IEEE Trans Pattern Anal Mach Intell* 6: 374–378.
- Goss, B.C., K.P. McGee, E.C. Ehman, A. Manduca, R.L. Ehman (2006) Magnetic resonance elastography of the lung: technical feasibility. *Magn Reson Med* 56: 1060–1066.
- Hut, P., J. Makino, S. McMillan (1995) Building a better leapfrog. *Astrophys J Lett* 443: 93–96.
- Ilyin, S.E., M.C. Flynn, C.R. Plata-Salaman (2001) Fiber-optic monitoring coupled with confocal microscopy for imaging gene expression in vitro and in vivo. *J Neurosci Methods* 108: 91–96.
- Ji, L., G. Danuser (2005) Tracking quasi-stationary flow of weak fluorescent signals by adaptive multi-frame correlation. *J Microsc* 220: 150–167.
- Kannus, P. (2000) Structure of the tendon connective tissue. *Scand J Med Sci Sports* 10: 312–320.
- Kauer, M., V. Vuskovic, J. Dual, G. Szekely, M. Bajka (2002) Inverse finite element characterization of soft tissues. *Med Image Anal* 6: 275–287.
- Lewa, C.J., M. Roth, L. Nicol, J.M. Franconi, J.D. de Certaines (2000) A new fast and unsynchronized method for MRI of viscoelastic properties of soft tissues. *J Magn Reson Imaging* 12: 784–789.
- Lopez, O., K.K. Amrami, A. Manduca, P.J. Rossman, R.L. Ehman (2007) Developments in dynamic MR elastography for in vitro biomechanical assessment of hyaline cartilage under high-frequency cyclical shear. *J Magn Reson Imaging* 25: 310–320.
- Machin, M., A. Santomaso, M. Mazzucato, M.R. Cozzi, M. Battiston, L. De Marco, P. Canu (2006) Single particle tracking across sequences of microscopical images: application to platelet adhesion under flow. *Ann Biomed Eng* 34: 833–846.
- Miura, K. (2005) Tracking movement in cell biology. *Adv Biochem Eng Biotechnol* 95: 267–295.
- Muthupillai, R., D.J. Lomas, P.J. Rossman, J.F. Greenleaf, A. Manduca, R.L. Ehman (1995) Magnetic resonance elastography by direct visualization of propagating acoustic strain waves. *Science* 269: 1854–1857.
- Ophir, J., I. Cespedes, H. Ponnekanti, Y. Yazdi, X. Li (1991) Elastography: a quantitative method for imaging the elasticity of biological tissues. *Ultrason Imaging* 13: 111–134.
- Othman, S.F., H. Xu, T.J. Royston, R.L. Magin (2005) Microscopic magnetic resonance elastography (microMRE). *Magn Reson Med* 54: 605–615.
- Plews, D.B., J. Bishop, A. Samani, J. Sclarretta (2000) Visualization and quantification of breast cancer biomechanical properties with magnetic resonance elastography. *Phys Med Biol* 45: 1591–1610.
- Pratt, W.K. (1991) *Digital Image Processing*. New York, Wiley.
- Rouviere, O., M. Yin, M.A. Dresner, P.J. Rossman, L.J. Burgart, J.L. Fidler, R.L. Ehman (2006) MR elastography of the liver: preliminary results. *Radiology* 240: 440–448.
- Rumian, A.P., A.L. Wallace, H.L. Birch (2007) Tendons and ligaments are anatomically distinct but overlap in molecular and morphological features – a comparative study in an ovine model. *J Orthop Res* 25: 458–464.
- Screen, H.R., D.A. Lee, D.L. Bader, J.C. Shelton (2003) Development of a technique to determine strains in tendons using the cell nuclei. *Biorheology* 40: 361–368.
- Screen, H.R., D.A. Lee, D.L. Bader, J.C. Shelton (2004) An investigation into the effects of the hierarchical structure of tendon fascicles on micromechanical properties. *Proc Inst Mech Eng [H]* 218: 109–119.
- Screen, H.R., J.C. Shelton, V.H. Chhaya, M.V. Kayser, D.L. Bader, D.A. Lee (2005) The influence of noncollagenous matrix components on the micromechanical environment of tendon fascicles. *Ann Biomed Eng* 33: 1090–1099.
- Shi, L.Z., J.M. Nascimento, M.W. Berns, E.L. Botvinick (2006) Computer-based tracking of single sperm. *J Biomed Opt* 11: 054009.
- Skovoroda, A.R., S.Y. Emelianov, M. O'Donnell (1995) Tissue elasticity reconstruction based on ultrasonic displacement and strain images. *IEEE Trans Ultrason Ferroelectr Freq Control* 42: 747–765.
- Snedeker, J.G., G. Pelled, Y. Zilberman, F. Gerhard, R. Muller, D. Gazit (2006) Endoscopic cellular microscopy for in vivo biomechanical assessment of tendon function. *J Biomed Opt* 11: 064010.
- Sumi, C., A. Suzuki, K. Nakayama (1995) Estimation of shear modulus distribution in soft tissue from strain distribution. *IEEE Trans Biomed Eng* 42: 193–202.
- Svanbro, A. (2004) In-plane dynamic speckle interferometry: comparison between a combined speckle interferometry/speckle correlation and an update of the reference image. *Appl Opt* 43: 4172–4177.
- Thitaikumar, A., R. Righetti, T.A. Krouskop, J. Ophir (2006) Resolution of axial shear strain elastography. *Phys Med Biol* 51: 5245–5257.
- Van Houten, E.E., K.D. Paulsen, M.I. Miga, F.E. Kennedy, J.B. Weaver (1999) An overlapping subzone technique for MR-based elastic property reconstruction. *Magn Reson Med* 42: 779–786.
- Wilson, C.A., J.A. Theriot (2006) A correlation-based approach to calculate rotation and translation of moving cells. *IEEE Trans Image Process* 15: 1939–1951.
- Wilson, L.S., D.E. Robinson, M.J. Dadd (2000) Elastography – the movement begins. *Phys Med Biol* 45: 1409–1421.
- Yang, F., M.A. Mackey, F. Ianzini, G. Gallardo, M. Sonka (2005) Cell segmentation, tracking, and mitosis detection using temporal context. *Med Image Comput Comput Assist Interv Int Conf Med Image Comput Comput Assist Interv* 8: 302–309.